Heavy Quark Fragmentation

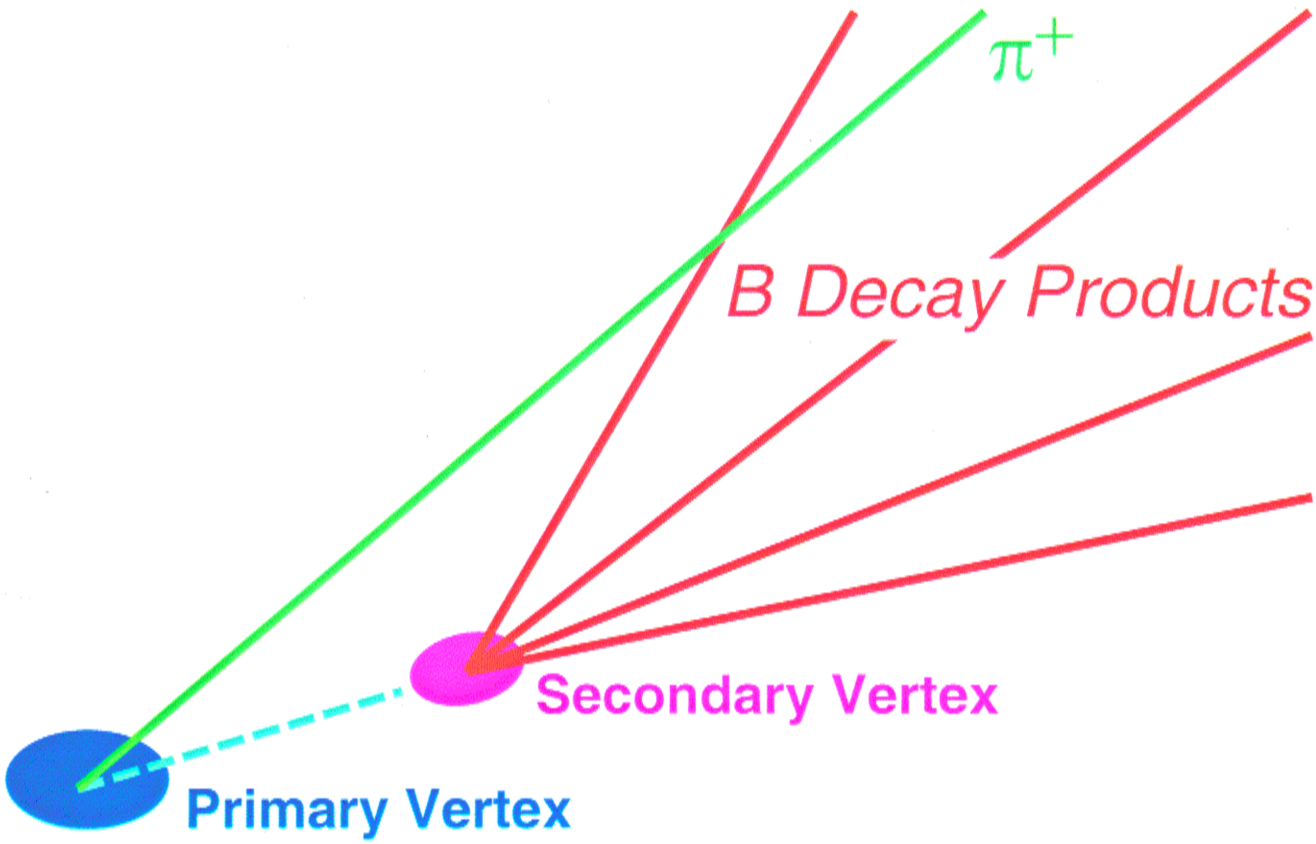

Scott Menary
York University
Toronto, Canada

37. HEAVY-QUARK FRAGMENTATION IN e^+e^- ANNIHILATION

Written January 1998 by D. Besson (University of Kansas).

Measurement of the fragmentation functions of heavy quarks provides information about non-perturbative particle production in a variety of experimental environments. The CDF observation of high p_T $J/\psi(1S)$ production rates far in excess of the extant theoretical predictions prompted the development of the color octet model (*e.g.*, $p\overline{p} \to gg \to \chi_c \to \psi + \mathrm{X}$) and highlighted the role of gluon fragmentation in charmonium production. Recent results from both LEP and HERA have also helped elucidate the gluonic contribution to charmed meson production. Current estimates from LEP are that gluon fragmentation accounts for approximately half of the D^* production in the lowest momentum region (the lowest quarter of the allowed kinematic region).

Many functional forms have been suggested to describe these momentum spectra for heavy quarks produced in e^+e^- annihilations. The functional form given by Peterson *et al.* [1] in terms of just one free parameter ϵ_P has found widespread use; other parameterizations are also given in the literature [2]. The earliest Peterson form was a function of one variable z, defined for a heavy-quark Q, light-quark $\overline{q}$ system as the ratio of the energy plus the longitudinal momentum of the hadron $Q\overline{q}$ to the sum of the energy and momentum of the heavy quark after accounting for initial state radiation, gluon bremsstrahlung, and final state radiation: $z = (E + p_{||})_{Q\overline{q}}/(E + p_Q)$. The main advantage of this variable is that it is relativistically invariant with respect to boosts in the direction of the primary quark. Unfortunately, as this quantity is not directly accessible, experiments typically use other scaling variables which are close approximations to z—either $x^+ = (p_{||} + E)_{\mathrm{hadron}}/(p_{||} + E)_{\mathrm{max}}$, $x_p = p/p_{\mathrm{max}}$, or $x_E = E_{\mathrm{hadron}}/E_{\mathrm{beam}}$.

The Peterson functional form is:

$$\frac{dN}{dz} = \frac{1}{z[1 - (1/z) - \epsilon_P/(1-z)]^2} \tag{37.1}$$

The bulk of the available fragmentation function data on charmed mesons (excluding $J/\psi(1S)$) is from measurements at $\sqrt{s} = 10$ GeV. Shown in Fig. 37.1 are the efficiency-corrected (but not branching ratio corrected) CLEO [3] and ARGUS [4] inclusive cross sections ($s \cdot \mathcal{B} d\sigma/dx_p$ in units of GeV^2-nb, with $x_p = p/p_{\mathrm{max}}$) for the production of pseudoscalar D^0 and vector D^{*+} in e^+e^- annihilations at $\sqrt{s} \approx 10$ GeV. For the D^0, $\mathcal{B}$ represents the branching fraction for $D^0 \to K^-\pi^+$; for the D^{*+}, $\mathcal{B}$ represents the product branching fraction: $D^{*+} \to D^0\pi^+; D^0 \to K^-\pi^+$. These inclusive spectra have not been corrected for cascades from higher states, nor for radiative effects. Note that since the momentum spectra are sensitive to radiative corrections, comparison of charm spectra at $\sqrt{s} = 10$ GeV cannot be compared directly with spectra at higher center-of-mass energies, and must be appropriately evolved.

Fits to the combined CLEO and ARGUS D^0 and D^{*+} data give $\epsilon_P(D^0) = 0.135 \pm 0.01$ and $\epsilon_P(D^*) = 0.078 \pm 0.008$; these are indicated in the solid curves. Measurement of the fragmentation functions for a variety of particles has allowed comparisons between mesons and baryons, and particles of different spin structure, as shown in Table 37.1

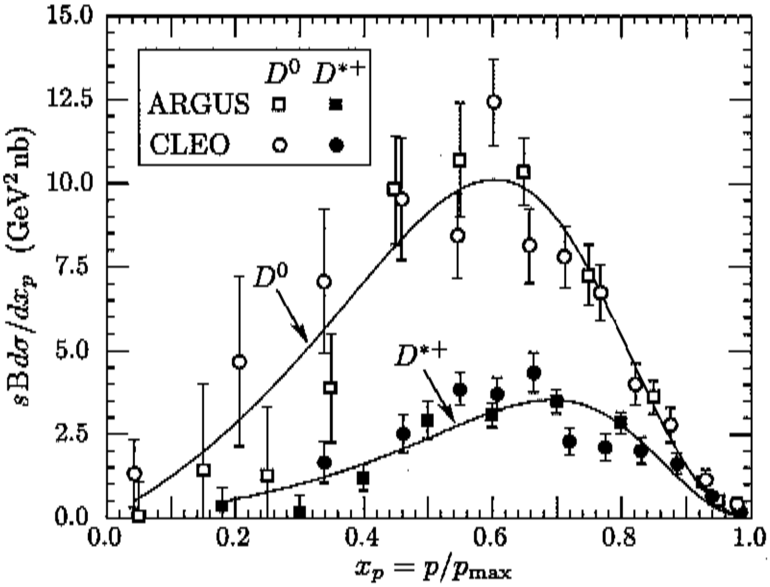

Figure 37.1: Efficiency-corrected inclusive cross section measurements for the production of D^0 and D^{*+} in e^+e^- measurements at $\sqrt{s} \approx 10$ GeV. The variable x_p is related to the Peterson variable z, but is not identical to it.

We note from Table 37.1 that the mass dependence of ϵ_P is less marked than the dependence on the orbital angular momentum structure of the charmed hadron being measured. Orbitally excited $L = 1$ charmed hadrons (D_J, $D_{s,J}$, and $\Lambda_{c,J}$) show consistently harder spectra (*i.e.*, smaller values of ϵ_P) than the $L = 0$ ground states, whereas the data for the ground state charmed baryons Λ_c and Ξ_c show agreement with the lighter (by $\approx$ 400–600 MeV) ground-state D and D_s charmed mesons. To some extent, the harder spectra of $L = 1$ hadrons can be attributed to the fact that all the $L = 1$ charmed hadrons will eventually decay into $L = 0$ hadrons.

Bottom-flavored hadrons at LEP have been measured to have an even harder momentum spectrum than charmed hadrons at lower energies [23–25]. Qualitatively, whereas charm spectra peak at $x_p \approx 0.6$, the spectra of bottom hadrons peak at $x_p \approx 0.8$. This is as expected in the Peterson model, where the value ϵ_P is expected to vary as the ratio of the effective light quark mass to the heavy quark mass in a heavy quark + light (di)quark hadron. In the case of charm, the Peterson functional form provides an acceptable description of the shape of the x_p distribution, provided the appropriate ϵ_P value is independently determined for each separate species of charmed particle. However, unlike charm, the numbers of fully reconstructed b-flavored hadrons is too small to allow a statistically compelling measure of ϵ_P for each separate bottom hadron. Consequently, a b-enriched sample is isolated kinematically, using, *e.g.*, a high p_T lepton and/or a displaced vertex to tag a primary b quark. The x_p distribution therefore includes all b-flavored hadrons in the sample, and does not yet allow a straightforward species-by-species ϵ_P extraction. Additional uncertainties in the case of bottom arise

Table 37.1: The Peterson momentum hardness parameter ϵ_P as obtained from $e^+e^- \to$ (particle) + X measurements.

Particle	L	$\sqrt{s}$	ϵ_P	Reference
D^0	0	10 GeV	0.135 ± 0.01	[3]
D^{*+}	0	10 GeV	0.078 ± 0.008	[3]
D_s^*	0	10 GeV	$0.04^{+0.03}_{-0.01}$	[5]
$D_1^0(2420)$	1	10 GeV	$0.034^{+0.018}_{-0.012}$	[6]
$D_2^0(2460)$	1	10 GeV	0.015 ± 0.004	[6]
$D_1^+(2420)$	1	10 GeV	$0.020^{+0.011}_{-0.006}$	[7]
$D_2^+(2460)$	1	10 GeV	0.013 ± 0.007	[7]
$D_{s1}(2536)$	1	10 GeV	$0.06^{+0.035}_{-0.03}$	[8]
$D_{s2}(2573)$	1	10 GeV	$0.027^{+0.043}_{-0.016}$	[9]
Λ_c	0	10 GeV	0.25 ± 0.03	[10,11]
Ξ_c	0	10 GeV	0.23 ± 0.05	[12,13]
Σ_c	0	10 GeV	0.29 ± 0.06	[14,15]
Σ_c^*	0	10 GeV	$0.30^{+0.10}_{-0.07}$	[16]
Ξ_c^{*+}	0	10 GeV	$0.24^{+0.22}_{-0.10}$	[17]
Ξ_c^{*0}	0	10 GeV	$0.22^{+0.15}_{-0.08}$	[18]
$\Lambda_{c,1}$	1	10 GeV	0.059 ± 0.028	[19,20]
$\Lambda_{c,2}$	1	10 GeV	0.053 ± 0.012	[19,21]
$\Xi_{c,2}$	1	10 GeV	$0.058^{+0.037}_{-0.021}$	[22]
b hadrons	—	90 GeV	$0.0047^{+0.0010}_{-0.0008}$	[23]

from the sensitivity of ϵ_P to the fragmentation model used to non-perturbatively evolve the initial $q\overline{q}$ system into final state hadrons.

In general, the b-quark fragmentation function distribution is found to be somewhat narrower than the shape of the Peterson function; this may be due to a systematic underestimate of soft gluon emission in event generators, and/or uncertainties in the appropriate mix of b-flavored hadrons. The match of a single Peterson function to data is therefore much more difficult for bottom than charm at this time, although there is relatively good agreement from experiment to experiment, as seen in Fig. 37.2, which displays the fragmentation function data from OPAL [23], ALEPH [24], and DELPHI [25].

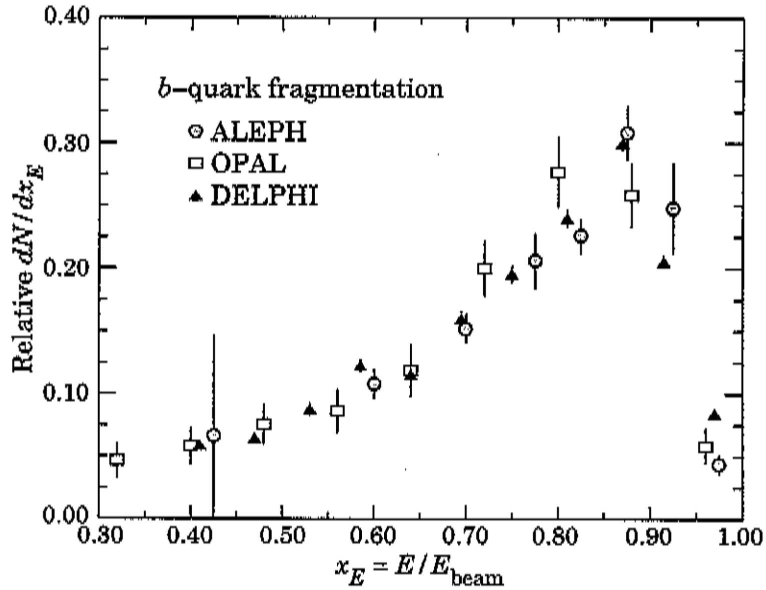

Figure 37.2: Fractional energy distribution for b-quark fragmentation for inclusive b production at LEP.

References:

1. C. Peterson, D. Schlatter, I. Schmitt, and P. M. Zerwas, Phys. Rev. **D27**, 105 (1983).
2. M.G. Bowler, Z. Phys. **C11**, 169 (1981);
   V.G. Kartvelishvili *et al.*, Phys. Lett. **B78**, 615 (1978);
   B. Andersson *et al.*, Z. Phys. **C20**, 317 (1983).
3. D. Bortoletto *et al.*, Phys. Rev. **D37**, 1719 (1988).
4. H. Albrecht *et al.*, Z. Phys. **C52**, 353 (1991).
5. J. A. McKenna, Ph.D. thesis, U. of Toronto, Toronto, Canada (1987), unpublished.
6. P. Avery *et al.*, Phys. Lett. **B331**, 236 (1994).
7. T. Bergfeld *et al.*, Phys. Lett. **B341**, 435 (1995).
8. R. Kutschke, presented at Intl. Conf. on Heavy Quark Physics, Ithaca, NY, 1989.
9. H. Albrecht *et al.*, Z. Phys. **C69**, 405 (1996).
10. G. Crawford *et al.*, Phys. Rev. **D45**, 752 (1992).
11. C. E. K. Charlesworth, A Study of the Decay Properties of the Charmed Baryon Λ_c^+, Ph. D. Thesis, University of Toronto (1992).
12. H. Albrecht *et al.*, Phys. Lett. **B247**, 121 (1990).
13. K. W. Edwards *et al.*, Phys. Lett. **B373**, 261 (1996).
14. H. Albrecht *et al.*, Phys. Lett. **B207**, 489 (1988).
15. T. Bowcock *et al.*, Phys. Rev. Lett. **62**, 2233 (1989).

of interest is from 2 to 2.5 GeV, it is natural to use 250 or 500 MeV bins. Unfortunately, 100 MeV bins leads to the the relative error on the number of D_s's per momentum bin getting too large[4]. It is clearly not possible to show all of the fits[5] but, just to show the quality of the fits, the results of fitting 4 $\varphi\pi$ distributions from cut set 4 are given in Figure 11. Throughout this note, the $m(\varphi\pi)$ histograms consist of 80 bins between 1.89 and 2.05 GeV. The 4 *yield VS momentum* spectra for cut set 4 (without the $\cos\theta^*_{TH}$ cut) are given in Figure 12.

6 Continuum Subtraction

It is clear from Figure 12 that, for $p(D_s) < 2$ GeV, there is very little systematic error associated with how the continuum is subtracted. It is also evident that the situation is exactly the opposite for the $b \to u$ momentum region of $2 < p(D_s) < 2.5$ GeV. This is illustrated in Figure 13 where Figure 12b, scaled by the relative luminosity factor of 2.2, has been superimposed on Figure 12d. Clearly, a bin by bin subtraction would only maximize the statistical error and would not be using all the information available (e.g., that the fragmentation function is assumed to be smooth).

Four different fragmentation functions were considered[6]:

1) A Gaussian function. There is no physical arguments for such a shape but, as we will see, it adequately describes some of the spectra, particularly those for R2GL below some cut.

2) The Peterson function;

$$F_P(x) = \frac{N}{x}\left(1 - \frac{1}{x} - \frac{\epsilon}{(1-x)}\right)^{-2} \quad (2)$$

3) The LUND symmetric fragmentation function;

$$F_L(x) = \frac{N}{x}(1-x)^a exp[-b/x] \quad (3)$$

4) A modified Peterson (hybrid) form;

$$F_h(x) = \frac{N}{x^\alpha}\left(1 - \frac{1}{x} - \frac{\epsilon}{(1-x)}\right)^{-4} \quad (4)$$

[4]This will certainly not be the case when it is possible to add in the 4s4 through 4s8 data sets.

[5]Since 250 MeV bins implies 5(*cut sets*) × 4(*per cut set*) × 20(*bins*) × 2(*with/without* $\cos\theta^*_{TH}$ *cut*) = 800 fits!.

[6]Here, $x = p/5$ since the spectra are plotted for $0 \le p \le 5$ GeV

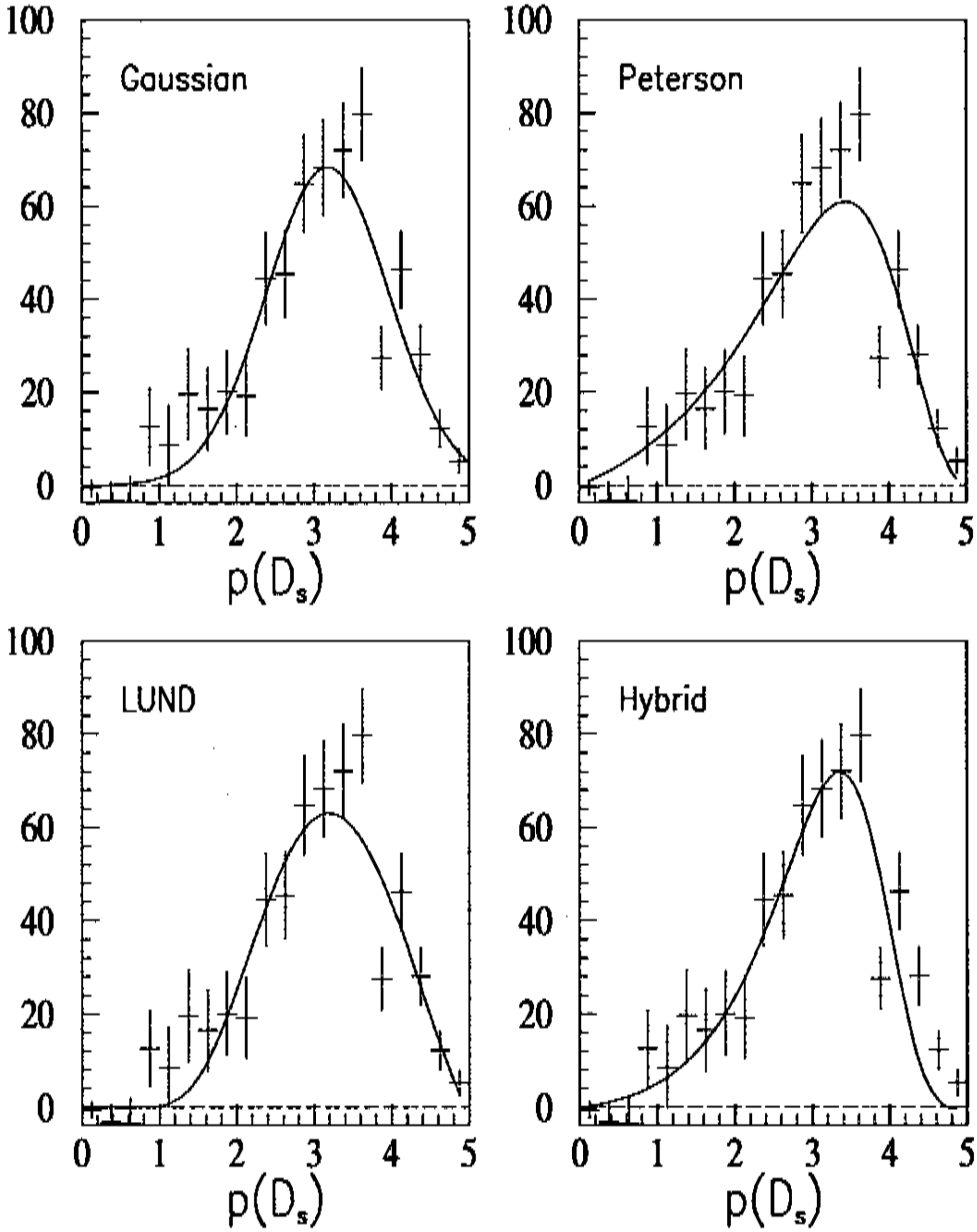

Figure 16: The results of fitting the continuum data D_s momentum spectra to four fragmentation functions. No R2GL cut has been applied.

Conclusions

- RAPGAP gives the best description
  .. but data show stronger η shift to the target region:
    - NLO effect (see HVQDIS NLO) ?
    - "Beam drag" from hadronisation?
    - Non-BGF charm source ?

- BGF mechanism describes "high" Q^2 (> 30 GeV^2); QPM/QCDC with active charm does't:

  ZM-VFN approach is not necessary even at $Q^2 >> m_c$!

- Data for η and P_0 disfavor the Peterson fragmentation

- Good agreement with HVQDIS can be achieved only after inclusion of RAPGAP fragmentation

- NLO gives better description for all distributions

- No evidence for intrinsic charm

- Second analysis is needed

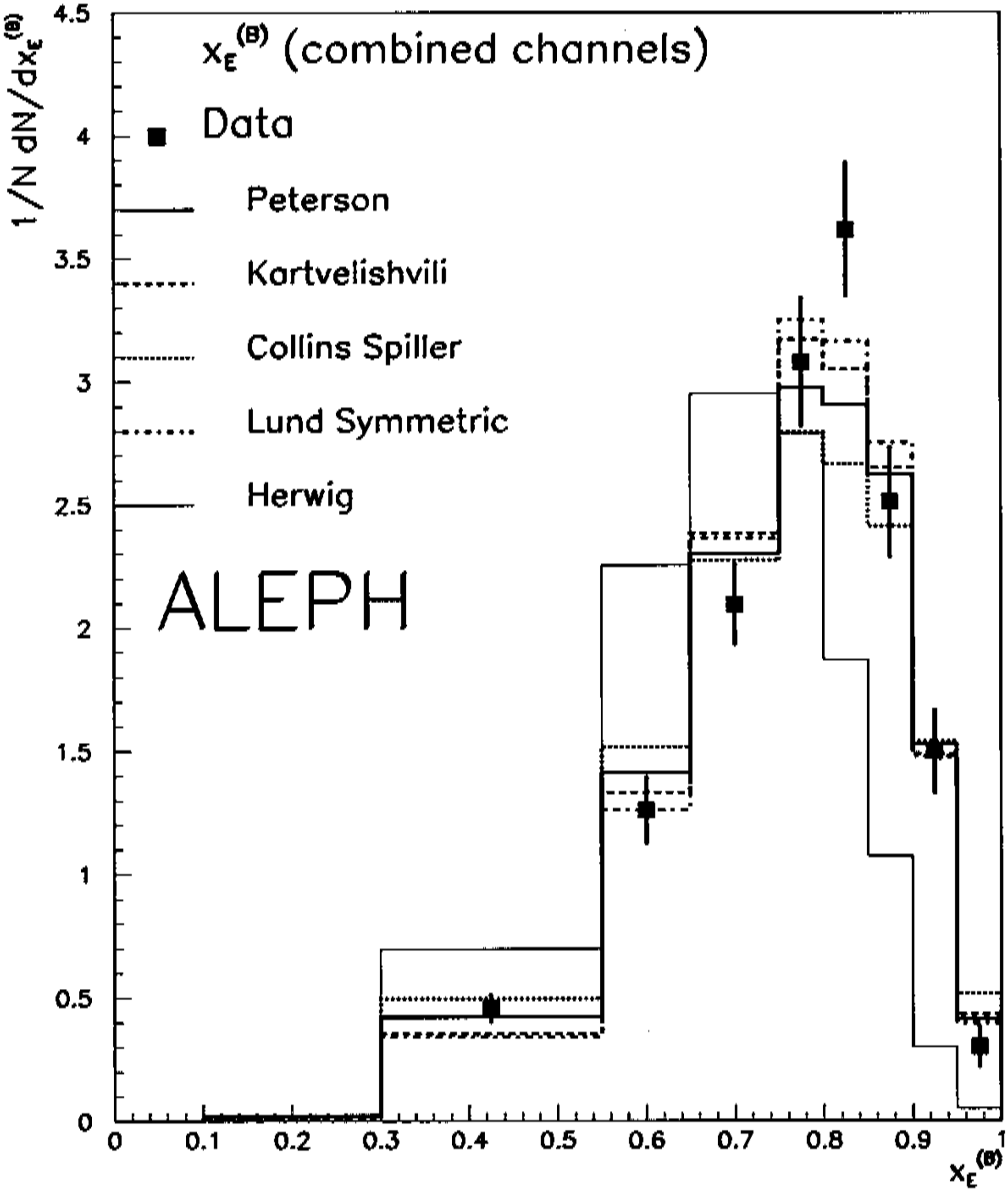

Figure 4: The measured scaled energy distribution of the reconstructed B mesons (before efficiency correction) combining all modes, compared to the predictions of different fragmentation models, for $f_{D^{**}} = 30\%$. The fragmentation parameters correspond to the best fit to the data; they are given in Table 3.

Channel	Weight	$\langle x_E^{(b)} \rangle$
$D^0 \to K\pi$:		
$B \to \ell\nu_\ell D^{*\pm}(X)$	28%	0.706 ± 0.012
$B \to \ell\nu_\ell D^0(X)$	33.3%	0.719 ± 0.012
$D^0 \to K\pi\pi\pi$:		
$B \to \ell\nu_\ell D^{*\pm}(X)$	14.8%	0.714 ± 0.017
$B \to \ell\nu_\ell D^0(X)$	9.0%	0.738 ± 0.025
$D^\pm \to K\pi\pi$:		
$B \to \ell\nu_\ell D^\pm(X)$	14.9%	0.706 ± 0.018
combined		0.715 ± 0.007

Table 2: The statistical weight of each channel and the mean $x_E^{(b)}$ of b-hadrons found for that channel. The mean $x_E^{(b)}$ is computed using the corrected data points for each channel, assuming $f_{D^{**}}$=30% and $f_{B^{**}}$=27.9%. Errors indicated are statistical only.

5.1 Comparison to fragmentation models

The measured $x_E^{(B)}$ distribution is compared to the prediction of different fragmentation models used in JETSET 7.3 [22] parton shower Monte Carlo with string fragmentation [21]. In this model, the fragmentation parameters are correlated with the QCD scale parameter Λ_{JETSET}, and with the shower cutoff mass M_{min}. From a comparison of the JETSET Monte Carlo to the ALEPH data [27], the values $\Lambda_{JETSET} = 311$ MeV and $M_{min} = 1.9$ GeV were determined. The following parametrizations of the fragmentation function were tried:

$$\text{Peterson et al. [1]} \quad D_b^H(z) \propto \frac{1}{z}\left(1 - \frac{1}{z} - \frac{\epsilon_b}{1-z}\right)^{-2} \tag{8}$$

$$\text{Kartvelishvili et al. [2]} \quad D_b^H(z) \propto z^{\alpha_b}(1-z) \tag{9}$$

$$\text{Collins and Spiller [3]} \quad D_b^H(z) \propto \left(\frac{1-z}{z} + \frac{(2-z)\epsilon_b}{1-z}\right)\left(1+z^2\right)\left(1 - \frac{1}{z} - \frac{\epsilon_b}{1-z}\right)^{-2} \tag{10}$$

$$\text{Lund symmetric [4]} \quad D_b^H(z) \propto \frac{1}{z}(1-z)^a exp(-0.5m_T^2/z) \tag{11}$$

The JETSET 7.3 Monte Carlo was used to convert these distributions into $x_E^{(b)}$ spectra. The data were also compared to the predictions of the cluster fragmentation model used in the HERWIG Monte Carlo [28], tuned to reproduce ALEPH data [27].

Monte Carlo events $B \to \ell\nu_\ell D^{(*)}X$ with full detector simulation were passed through the same analysis chain as the data and the reconstructed $x_E^{(B)}$ distribution of the real events was compared to that of the selected Monte Carlo events. A simulation of the different fragmentation functions was obtained from reweighting events according to the z distributions predicted for the various models. To reach the best statistical sensitivity, the five decay channels used

- D^{**} fraction in B semileptonic decays: the systematic error due to the uncertainty on $f_{D^{**}}$ was estimated by repeating the analysis for a variation $\Delta f_{D^{**}} = \pm 0.1$, as expected from a study of recent experimental results [23, 24, 25, 26]. The systematic error on the mean $x_E^{(b)}$ is $\Delta\langle x_E^{(b)}\rangle = \pm 0.010$

- D^{**} model: while there is clear experimental evidence for the decay $B \rightarrow \ell^{\pm}\nu_{\ell}D^{**}_{2420}$ [23, 25, 26], other unidentified semileptonic B decays could either include heavier resonant states D_J^{**}[26] or non-resonant decays $B \rightarrow \ell^{\pm}\nu_{\ell}D^{(*)}\pi$[25]. For the latter, the energy carried by the missing π is expected to be about 10% higher than in resonant decays. The corresponding uncertainty on $x_E^{(b)}$ is $\Delta\langle x_E^{(b)}\rangle = \pm 0.002$

- D^*/D ratio: this ratio can affect the result by changing the fraction of $B \rightarrow \ell\nu_{\ell}D^{*0}$ decays in the sample of $B \rightarrow \ell\nu_{\ell}D^0$ (X) events. By changing this ratio from 3 to 2, a variation of the mean $x_E^{(b)}$ $\Delta\langle x_E^{(b)}\rangle = 0.001$ is obtained.

- B^{**} fraction in B semileptonic decays: from [29], the uncertainty on $f_{B^{**}}$ is estimated to ± 0.072. The corresponding uncertainty on the mean $x_E^{(b)}$ of the leading b-hadron produced in the b-quark hadronization is $\Delta\langle x_E^{(b)}\rangle = \pm 0.004$

- B^{**} model: the estimated uncertainty on the mean mass of B^{**} states produced is ± 20 MeV/c^2 [29]. The corresponding uncertainty on the mean $x_E^{(b)}$ is $\Delta\langle x_E^{(b)}\rangle = \pm 0.001$. Other modelling uncertainties (B^{**} width, angular distribution of decay products) have an even smaller effect.

- Background subtraction: this background comes from all processes (but primary semileptonic B decays) leading to a reconstructed lepton correlated to a D meson in the same hemisphere. From the uncertainty on the branching ratios $B \rightarrow D_s\bar{D}(X)$ and the statistical error on the Monte Carlo sample, a $\pm 70\%$ error on this background was assigned. The corresponding variation of $x_E^{(b)}$ is $\Delta\langle x_E^{(b)}\rangle = \pm 0.002$

- Neutrino energy reconstruction: the hemisphere energy reconstruction was checked by computing the neutrino energy in each hemisphere (according to Eq. 6 and 7) for an inclusive sample of events containing a high transverse momentum lepton with $p_T > 1$ GeV/c. It can be seen from Fig. 5 that the neutrino energy distribution for the data is rather well reproduced by the simulation, both for the lepton hemisphere, in which a neutrino is always expected, and for the opposite hemisphere: no significant shift is observed and the detector resolution is correctly simulated. The precision on the neutrino energy calibration is therefore estimated to be 100 MeV, from which a systematic uncertainty $\Delta\langle x_E^{(b)}\rangle = 0.002$ on $x_E^{(b)}$ results.

- Uncertainty on the number of events extrapolated in the bin $x_E^{(b)} < 0.3$ and choice of the parametrization curve $f(x_E^{(b)})$: since $f(x_E^{(b)})$ is used both for the correction and to

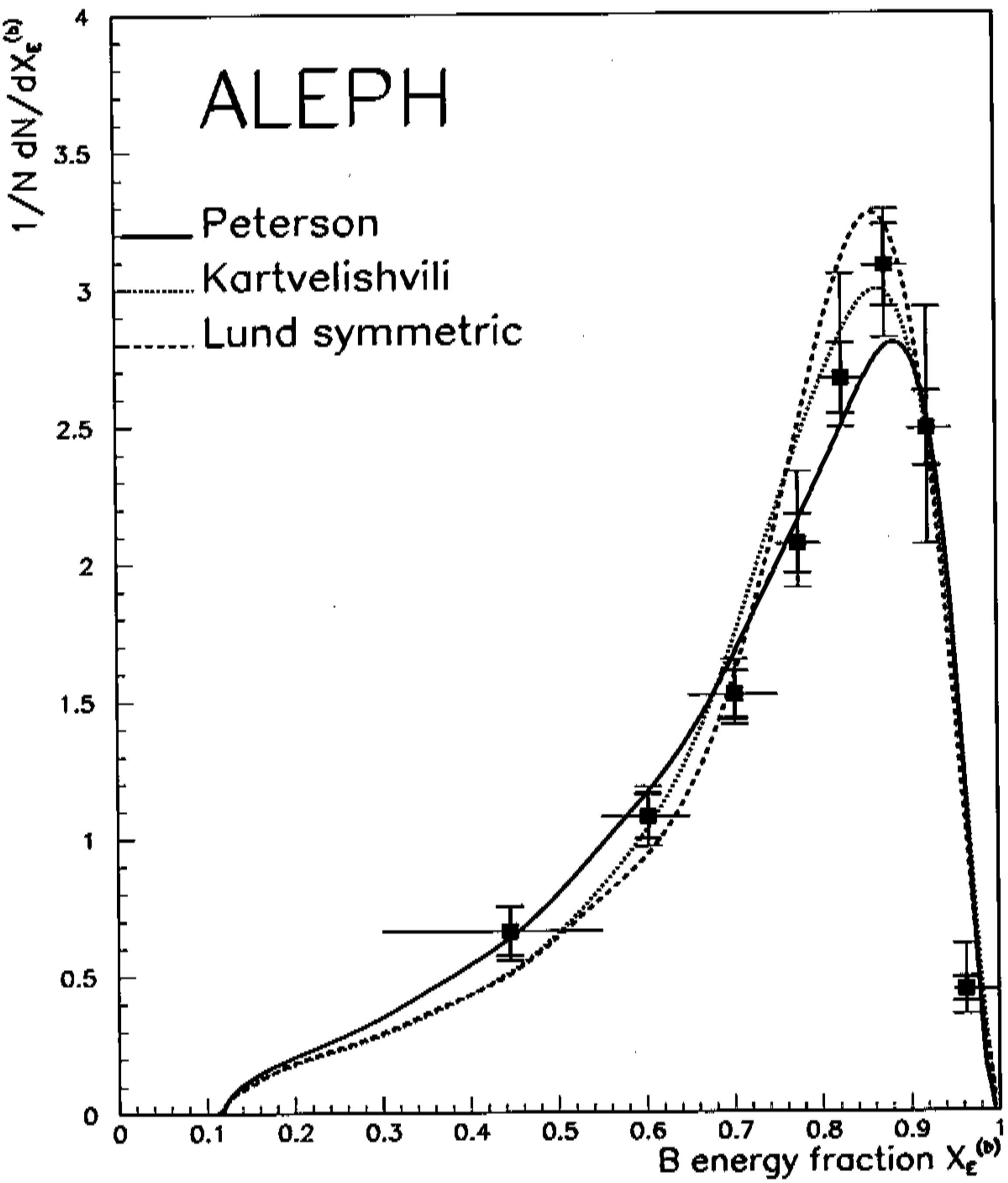

Figure 7: The acceptance corrected $x_E^{(b)}$ spectrum of the leading b-meson for $f_{B^{**}}$=27.9% and $f_{D^{**}}$=30%, compared with the predictions of different fragmentation models. The smaller error bar is statistical. The larger one is the sum of statistical + systematic errors. The errors shown do not account for the point-to-point correlations induced by the deconvolution process.

ALEPH data seems more peaked (B^{**} correction?). It would be useful to clarify all this within the end of the workshop

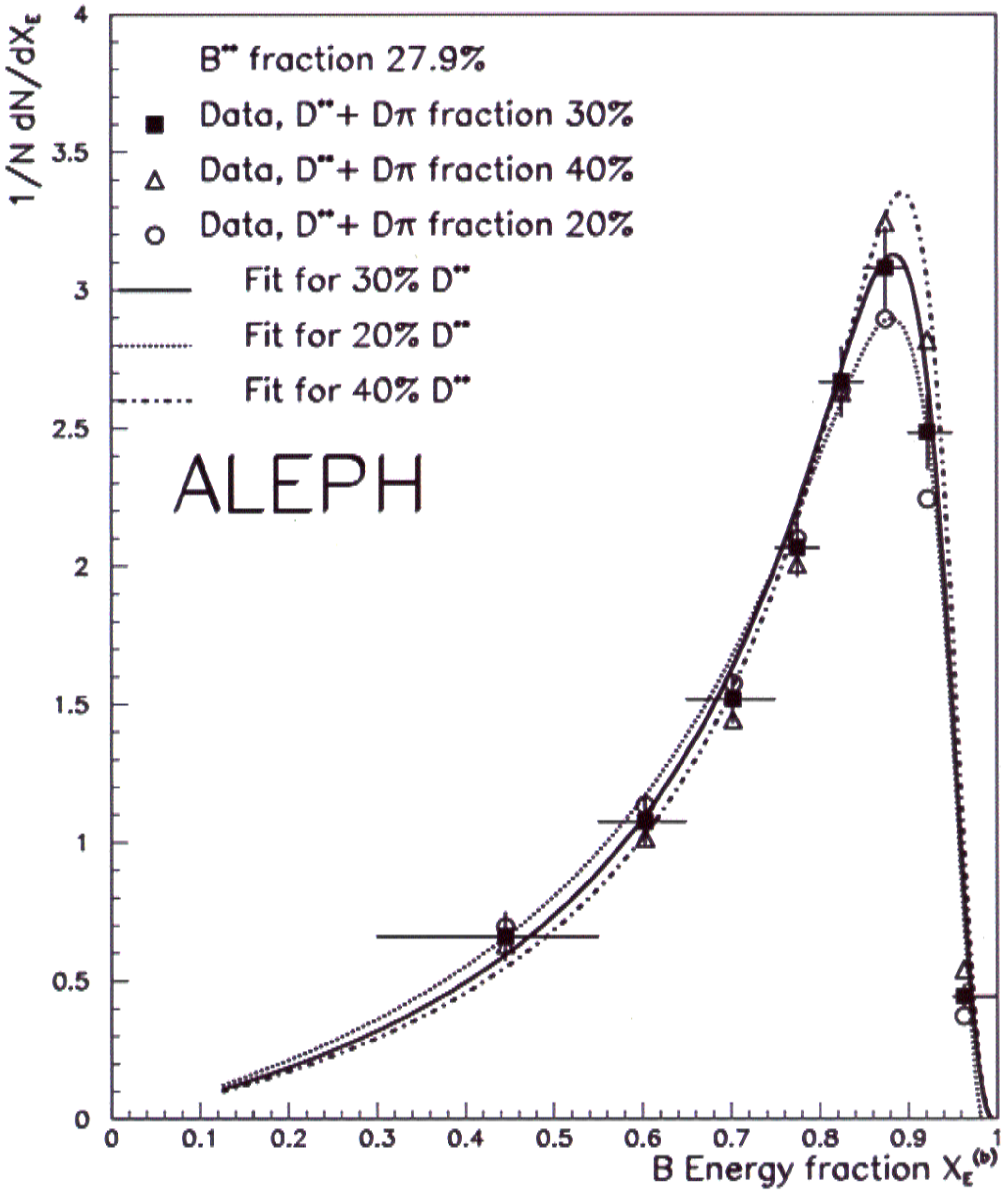

Figure 6: The acceptance corrected $x_E^{(b)}$ spectrum of the leading b-mesons combining all channels, for $f_{D^{**}}$=20, 30 and 40%. The error shown is statistical only and does not account for the point-to-point correlations induced by the deconvolution process. It is only shown for $f_{D^{**}}$=30%. Also shown are the fit results of Eq. 16 for $f_{D^{**}}$=20, 30 and 40%.

hep-ex/9908032 6 Aug 1999

SLAC–PUB–8153
June 1999

Measurement of the b Quark Fragmentation Function in Z^0 decays*

The SLD Collaboration**
Stanford Linear Accelerator Center
Stanford University, Stanford, CA 94309

ABSTRACT

We present preliminary results of a new measurement of the inclusive b quark fragmentation function in Z^0 decays using a novel kinematic B hadron energy reconstruction technique. The measurement is performed using 150,000 hadronic Z^0 events recorded in the SLD experiment at SLAC between 1996 and 1997. The small and stable SLC beam spot and the CCD-based vertex detector are used to reconstruct topological B-decay vertices with high efficiency and purity, and to provide precise measurements of the kinematic quantities used in this technique. We measure the B energy with good efficiency and resolution over the full kinematic range. We compare the measured scaled B hadron energy distribution with several functional forms of the B hadron energy distribution and predictions of several models of b quark fragmentation. Several functions are excluded by the data. The average scaled energy of the weakly decaying B hadron is measured to be $x_B = 0.714 \pm 0.005$ (stat) ± 0.007 (syst) ± 0.002 (model) (preliminary).

Contributed to: the International Europhysics Conference on High Energy Physics, 15-21 July 1999, Tampere, Finland, Ref. 1_185, and to the XIXth International Symposium on Lepton and Photon Interactions, August 9-14 1999, Stanford, USA.

* Work supported by Department of Energy contract DE-AC03-76SF00515 (SLAC).

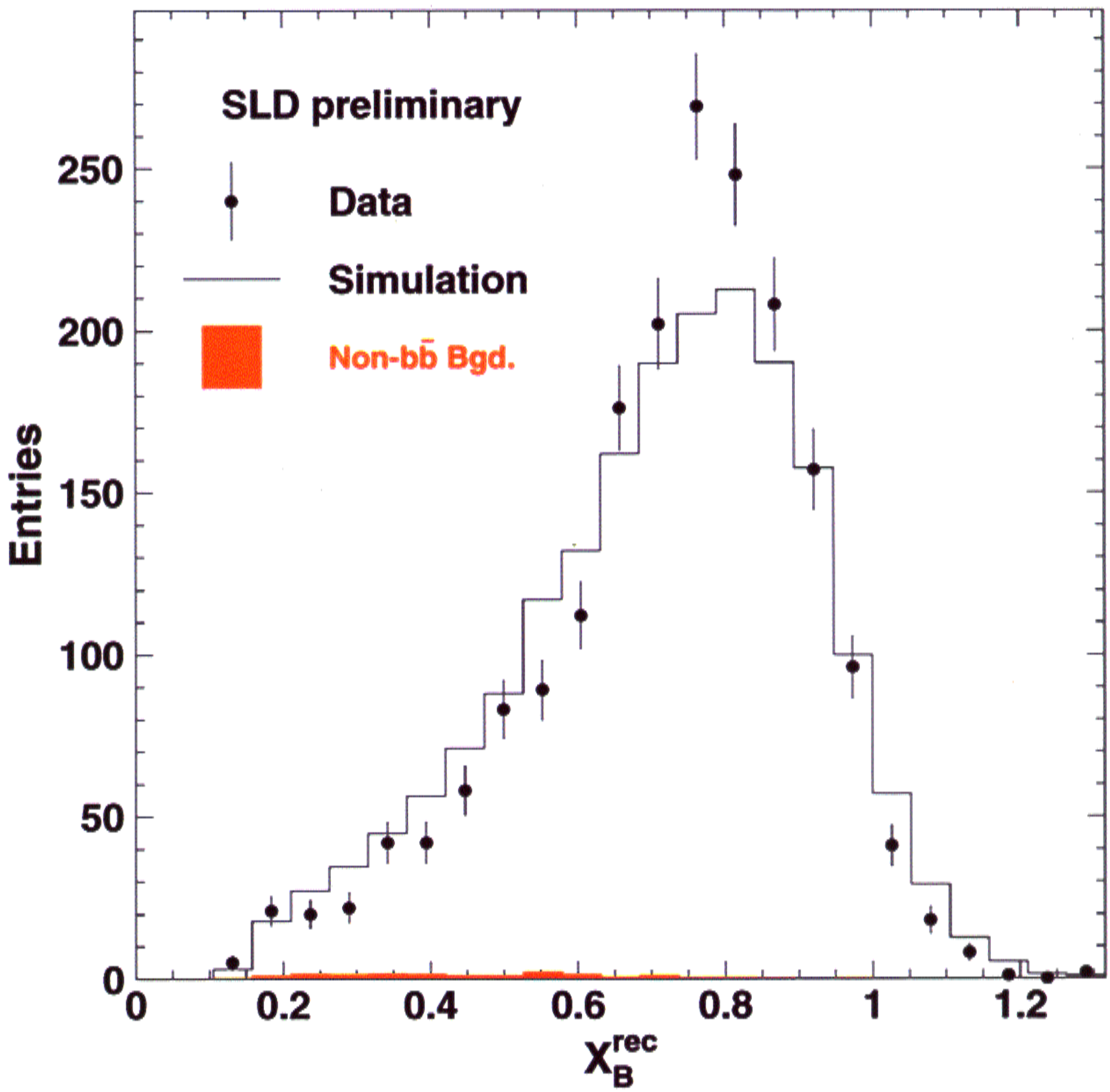

Figure 7: Distribution of the reconstructed scaled B hadron energy for 1996-97 data (points) and the default Monte Carlo simulation (histogram). The solid histogram shows the non-$b\bar{b}$ background.

Function	$D(x)$	Reference
ALEPH 1	$\frac{1-x}{x}(1-\frac{c}{x}-\frac{d}{1-x})^{-2}$	[12]
ALEPH 2	$\frac{1}{x}(1-\frac{c}{x}-\frac{d}{1-x})^{-2}$	[12]
BCFY	$\frac{x(1-x)^2}{[1-(1-r)x]^6}[3+\sum_{i=1}^{4}(-x)^i f_i(r)]$	[4]
Collins and Spiller	$(\frac{1-x}{x}+\frac{(2-x)\epsilon_b}{1-x})(1+x^2)(1-\frac{1}{x}-\frac{\epsilon_b}{1-x})^{-2}$	[10]
Kartvelishvili *et al.*	$x^{\alpha_b}(1-x)$	[6]
Lund	$\frac{1}{x}(1-x)^a exp(-bm_\perp^2/x)$	[9]
Peterson *et al.*	$\frac{1}{x}(1-\frac{1}{x}-\frac{\epsilon_b}{1-x})^{-2}$	[8]
Polynomial	$x(1-x)(1+\sum_{i=1}^{5}p_i x^i)$	(see text)
Power	$x^\alpha(1-x)^\beta$	(see text)

Table 1. Fragmentation functional forms used in comparison with the data. For the BCFY function $f_1(r) = 3(3-4r)$, $f_2(r) = 12-23r+26r^2$, $f_3(r) = (1-r)(9-11r+12r^2)$, and $f_4(r) = 3(1-r)^2(1-r+r^2)$. A polynomial function and a power function are also included.

Function	χ^2/dof	Parameters	$\langle x_B \rangle$
ALEPH 1	15.2/15	$c = 0.860^{+0.019}_{-0.018}$	0.718±0.005
		$d = 0.019 \pm 0.002$	
ALEPH 2	23.7/15	$c = 0.938^{+0.039}_{-0.034}$	0.720±0.005
		$d = 0.036 \pm 0.002$	
BCFY	52.3/16	$r = 0.2316^{+0.0092}_{-0.0088}$	0.713±0.005
Collins and Spiller	54.3/16	$\epsilon_b = 0.044^{+0.005}_{-0.004}$	0.714±0.005
Kartvelishvili *et al.*	79.6/16	$\alpha_b = 4.15 \pm 0.11$	0.720±0.004
Lund	139.1/15	$a = 2.116^{+0.118}_{-0.114}$	0.720±0.005
		$bm_\perp^2 = 0.408^{+0.073}_{-0.070}$	
Peterson *et al.*	26.0/16	$\epsilon_b = 0.0338^{+0.0020}_{-0.0022}$	0.719±0.005
Polynomial	14.4/12	$p_1 = -12.4 \pm 0.4$	(see text)
		$p_2 = 58.7 \pm 1.9$	
		$p_3 = -130.5 \pm 4.2$	
		$p_4 = 136.8 \pm 4.3$	
		$p_5 = -53.7 \pm 1.8$	
Power	78.5/15	$\alpha = 3.91^{+0.25}_{-0.24}$	0.722±0.005
		$\beta = 0.894^{+0.102}_{-0.097}$	

Table 2. Results of the χ^2 fit of fragmentation functions to the reconstructed B hadron energy distribution after background subtraction. Minimum χ^2, number of degrees of freedom and coresponding parameter values are listed. Errors are statistical only.

4. Tests of Functional Forms and Models

After background subtraction, the distribution of the reconstructed scaled B hadron energy is compared with a set of *ad hoc* functional forms of the x_B distribution in order to estimate the variation in the shape of the x_B distribution. For each functional form, the default SLD Monte Carlo is re-weighted and then compared with the data bin-by-bin and a χ^2 is computed. The minimum χ^2 is found by varying the input parameter(s). The Peterson function [8], two *ad hoc* generalizations of the Peterson function[12] (ALEPH 1 and 2) and a 7th-order polynomial * are consistent with the data. We exclude the functional forms described in BCFY [4], Collins and Spiller [10], Kartvelishvili [6], Lund [9] and a power function of the form $f(x) = x^\alpha(1-x)^\beta$. The result is shown in Figure 6 and in Table 1 and 2.

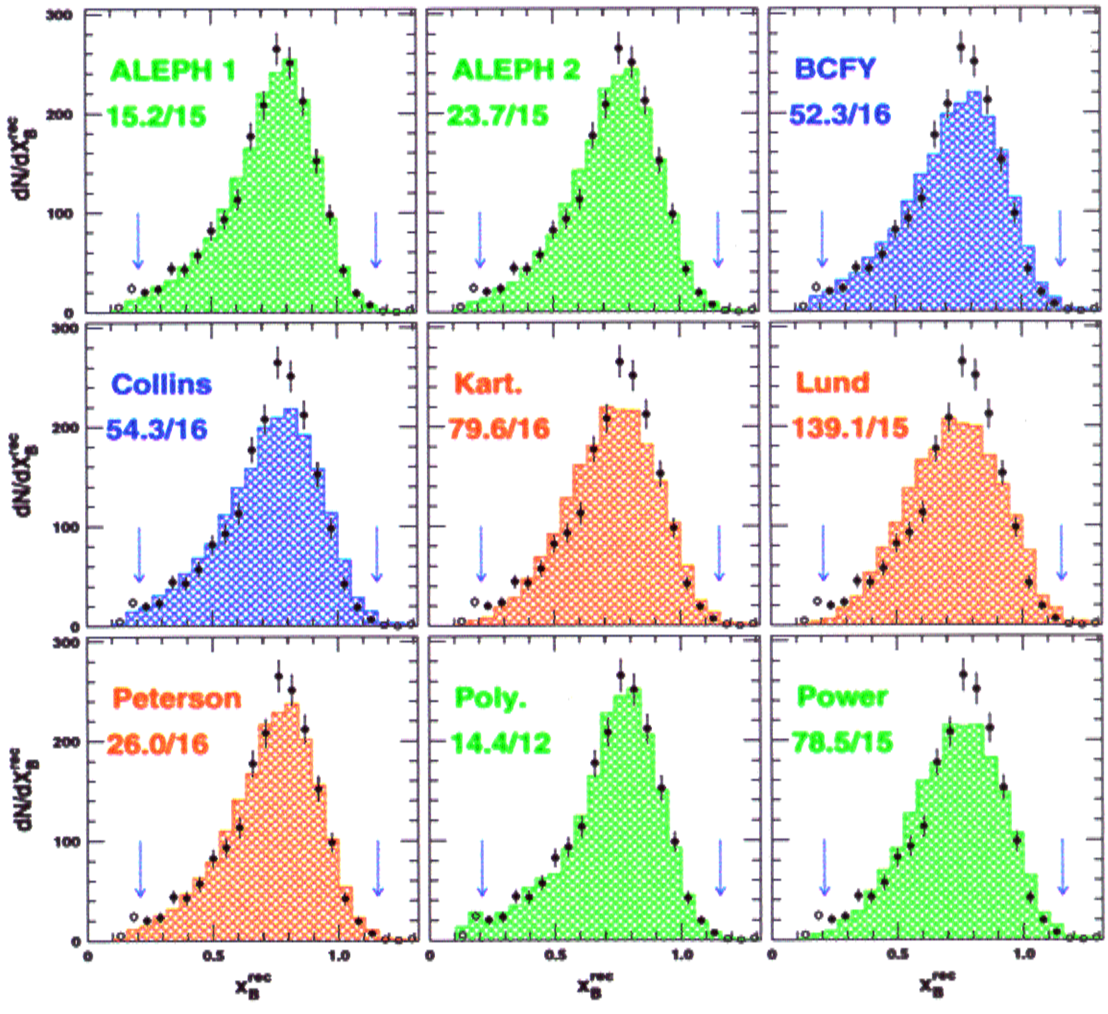

Figure 7. Each figure shows the background-subtracted distribution of reconstructed B hadron energy for the data (points) and for the simulation (histograms) based on the respective optimised input fragmentation function. The χ^2 fit uses data in the bins between the two arrows.

*The behavior of this polynomial is rather unphysical at low x_B and will not be considered hereafter

Other relevant systematic effects such as variation of the event selection cuts and the assumed B hadron mass are also found to be very small. As a cross-check, we vary the M_{0max} cut (Equation (8)) in selecting the final B sample within a large range and repeat the analysis procedure. In each case, conclusions about the shape of the B energy distribution hold. In each bin, all sources of systematic uncertainty are added in quadrature to obtain the total systematic error.

7. Summary and Conclusions

We have used the excellent tracking and vertexing capabilities of SLD to reconstruct the energies of B hadrons in $e^+e^- \rightarrow Z^0$ events over the full kinematic range by applying a new kinematic technique to an *inclusive* sample of topologically reconstructed B hadron decay vertices. The overall B selection efficiency of the method is 3.9%. We estimate the resolution on the B energy to be about 10.4% for roughly 83% of the reconstructed decays. The energy resolution for low energy B hadrons is significantly better than previous measurements.

In order to get a good estimate of the model dependence of the unfolded distribution, the distribution of reconstructed scaled B hadron energy, $D^{data}(x_B^{rec})$, is compared **case 1)** with predictions of *either* perturbative QCD and phenomenological b quark fragmentation models in the context of the JETSET parton shower Monte Carlo, *or* HERWIG and UCLA fragmentation models, and **case 2)** with a set of functional forms for the B energy distribution. In **case 1)**, the Lund and the Bowler models are consistent with the data; the model of Kartvelishvili *et al.* is in marginal agreement with the data. The models based on the perturbative QCD calculations of Braaten *et al.*, and of Collins and Spiller, and the Peterson model are disfavored by the data. Although both versions of the HERWIG model are excluded by the data, the new version is very much improved. The UCLA model describes the data reasonably well. In **case 2)**, four functional forms, namely the two generalised Peterson functions F1 and F2, the Peterson function, and a constrained 8th-order polynomial are found to be consistent with the data.

The raw B energy distribution is then corrected for bin-to-bin migrations caused by the resolution of the method and for selection efficiency to derive the energy distribution of the weakly decaying B hadrons produced in Z^0 decays. Systematic uncertainties in the correction have been evaluated and are found to be significantly smaller than those of previous direct B energy measurements. The final corrected x_B distribution $D^{data}(x_B^{true})$ is shown in Figure 11. The statistical and unfolding uncertainties are indicated separately.

It is conventional to evaluate the mean of this B energy distribution, $< x_B >$. For each of the eight functions providing a reasonable description of the data (four from **case 1)** and four from **case 2)**), we evaluate $< x_B >$ from the distribution that corresponds to the optimised parameters; these are listed in Table 2 and Table 4. We take the average of the eight values of $< x_B >$ as our central value, and define the model-dependent uncertainty to be the r.m.s. deviation within each bin. All detector

DØ Note: 3430
April 25th, 1998

Tuning of the b-Quark Fragmentation in ISAJET

Marc M. Baarmand, Frédéric Stichelbaut

State University of New York at Stony Brook

Abstract

The parameter used in ISAJET to describe the fragmentation of the b-quark with the Peterson function, XGEN(5), has been tuned with data recently obtained by the ALEPH experiment at LEP. We obtain a value XGEN(5) $= 0.44^{+0.15}_{-0.11}$. We also studied the influence of the b-quark fragmentation on the b-produced muon spectrum.

1 Introduction

The fragmentation of b quarks into B hadrons is usually described by the Peterson fragmentation function [1], which has the form:

$$f(z) \propto \frac{1}{z}\left(1 - \frac{1}{z} - \frac{\epsilon_b}{1-z}\right)^{-2}. \quad (1)$$

In this function, z is the fraction of the parton energy retained by the B hadron when the b quark undergoes hadronisation and is defined:

$$z = \frac{(E + p_{\parallel})_{hadron}}{(E + p_{\parallel})_{quark}}. \quad (2)$$

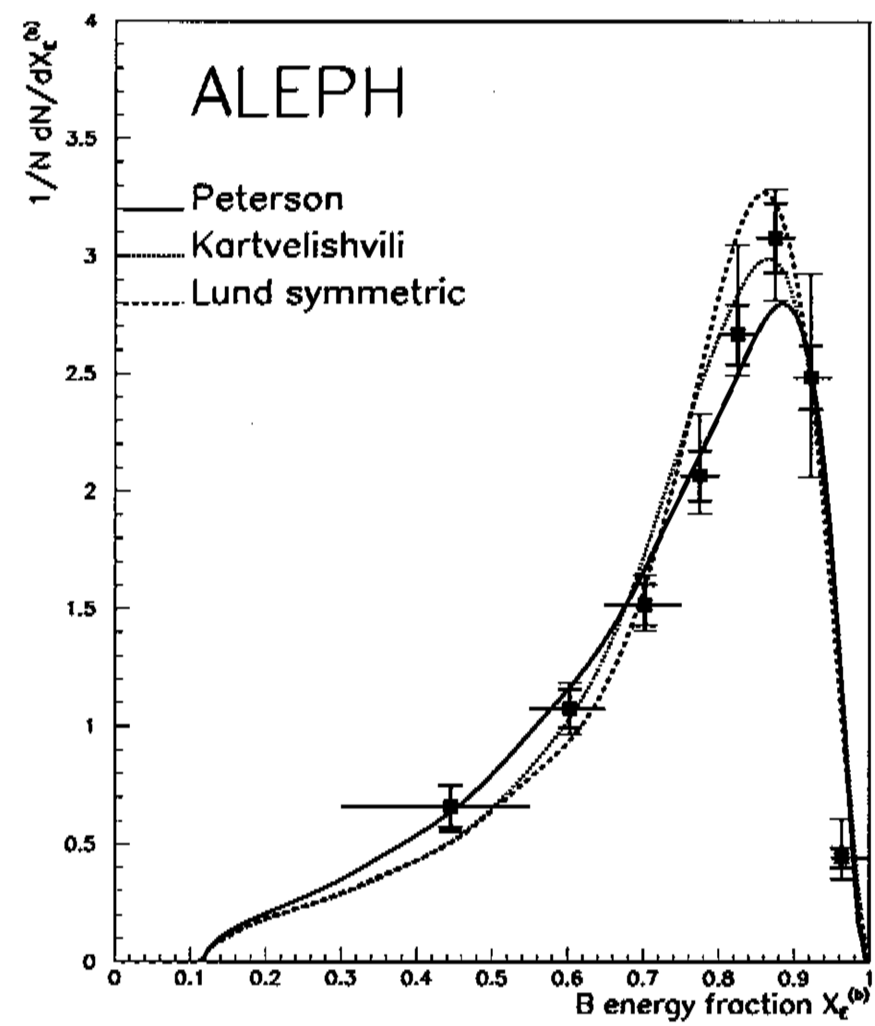

Figure 1: The $x_E^{(b)}$ spectrum of the leading b-meson measured by ALEPH and compared with the predictions of different fragmentation models. The errors are the sum of the statistical and systematic errors.